

Spatial adiabatic passage via interaction-induced band separation

Albert Benseny,^{*} Jérémie Gillet, and Thomas Busch

Quantum Systems Unit, OIST Graduate University, Onna, Okinawa 904-0495, Japan

(Dated: February 25, 2016)

The development of advanced quantum technologies and the quest for a deeper understanding of many-particle quantum mechanics requires control over the quantum state of interacting particles to a high degree of fidelity. However, the quickly increasing density of the spectrum, together with the appearance of crossings in time-dependent processes, makes any effort to control the system hard and resource intensive. Here we show that in trapped systems regimes can exist, in which isolated energy bands appear that allow to easily generalize known single-particle techniques. We demonstrate this for the well-known spatial adiabatic passage effect, which can control the center-of-mass state of atoms with high fidelity.

PACS numbers: 03.75.Lm, 03.75.Be, 42.50.Dv

I. INTRODUCTION

Understanding the effects of interactions between many particles at the quantum level is an important task for increasing the access to, and control over, ever larger parts of the Hilbert space [1, 2]. However, this is a difficult problem, as interacting many-particle states are usually too complex to allow for exact analytical treatment and often require numerical resources that are out of reach for current computers. One way to approach this problem is to study small systems first and use the developed understanding for scaling up. This allows theoretical treatment and experimental verification, as recent progress in cold atomic gases has led to control over the trapping of small numbers of particles and the ability to measure them with high precision [3]. Using Feshbach resonances one can then change the interaction strength between the particles and engineer well-defined quantum states. The importance of this lies in the ability to explore new aspects of fundamental quantum mechanics as well as to design new applications in quantum technologies.

However, no generic and straightforward strategies exist to develop new engineering tools that take advantage of the full Hilbert space. One controlled way to make progress is to try to generalize known techniques for single-particle states to either weakly-correlated many-body states or to small strongly-correlated systems [4]. In this work we focus on the well-known spatial adiabatic passage (SAP) protocol [5–8], which is a technique that allows to transfer a localized wave function between different positions in space by adiabatically following a specific energy eigenfunction. SAP for ultracold atoms has up to now only been studied for a single atom [5, 9–11], weakly-interacting systems [12–15], or fermionized bosons [16]. Here we discuss a system of two interacting bosons in a triple well potential and, using exact solutions and Hubbard models, we show that the interactions

can destroy, but also revive, the possibility for SAP due to an interaction-induced energy-band separation. This separation allows to generalize single-particle processes to multiple particles and requires to consider repulsively-bound pair co-tunnelling processes [17–24].

In the following we will first very briefly review the technique of spatial adiabatic passage (Section II) and the general solution for two interacting particles in a harmonic trap (Section III). We then numerically solve the problem of SAP for interacting particles (Section IV) and discuss the limiting cases for weak and strong interactions using the Hubbard model (Sections V and VI). The importance of level crossings and non-adiabatic evolution is discussed in Section VII before we conclude.

II. SINGLE-PARTICLE SAP

The SAP protocol for a single atom involves three degenerate localized trapping states $|j\rangle$ with $j = l, m$ and r (for left, middle and right), which are centered at positions $d_L < d_M < d_R$. The system is described by the Hamiltonian

$$H_0 = \Omega_{LM}|l\rangle\langle m| + \Omega_{MR}|m\rangle\langle r| + \text{h.c.}, \quad (1)$$

where the time-dependent nearest-neighbor couplings $\Omega_{jj'}$ are controlled by the distance between the traps [5]. Note that throughout the paper we use dimensionless units where \hbar , atomic masses, and trapping frequencies are equal to 1. One of the eigenstates of H_0 is the so-called *dark state* [25],

$$|D\rangle = \cos\theta|l\rangle - \sin\theta|r\rangle, \quad (2)$$

with $\tan\theta = \Omega_{LM}/\Omega_{MR}$ and SAP describes the transport of a particle from $|l\rangle$ to $|r\rangle$ following $|D\rangle$ by changing θ from 0 ($\Omega_{MR} \gg \Omega_{LM}$) to $\pi/2$ ($\Omega_{MR} \ll \Omega_{LM}$). This is achieved with the trap movement shown in Fig. 1(a), which maintains an energy gap between the dark state and the two other eigenstates of the order of $\sqrt{\Omega_{LM}^2 + \Omega_{MR}^2}$ (see Fig. 1(b)) and changes the dark state from $|l\rangle$ at $t = 0$ to $|r\rangle$ at final time $t = T$ (see Fig. 1(c)).

^{*} albert.benseny-cases@oist.jp

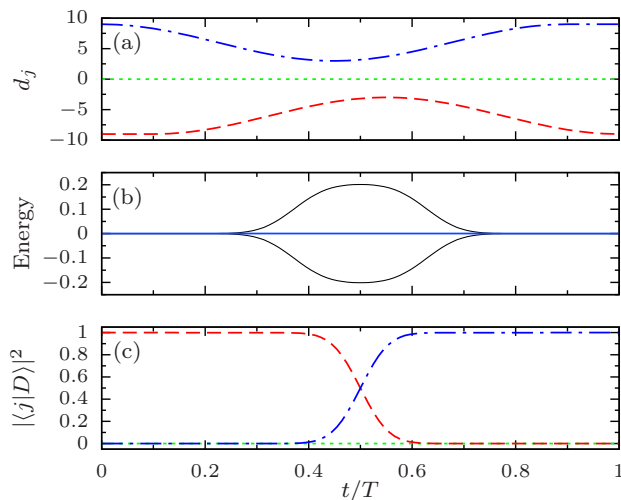


FIG. 1. (Color online) (a) Positions of the three harmonic well minima for the SAP protocol as used in our simulations (dashed red: d_L , dotted green: d_M , dot-dashed blue: d_R). The initial (and final) distance between wells is $d_{\max} = 9$, the minimum distance is $d_{\min} = 3$ and the time delay between the two approaches is $T/10$. (b) Energy eigenvalues of the single-particle Hamiltonian (1), with the one corresponding to $|D\rangle$ displayed in blue (gray). (c) Coefficients of $|D\rangle$ in the $\{|j\rangle\}$ basis (dashed red: $|l\rangle$, dotted green: $|m\rangle$, dot-dashed blue: $|r\rangle$).

To avoid excitations and ensure that SAP succeeds, the whole process needs to be carried out adiabatically.

III. EXACT MODEL FOR TWO PARTICLES

For simplicity, we will use a one-dimensional model of two interacting bosons in a triple-well potential, even though our results can easily be extended to higher dimensions. The Hamiltonian is then given by

$$H = \sum_{k=1}^2 \left(-\frac{1}{2} \frac{\partial^2}{\partial x_k^2} + V(x_k, t) \right) + g\delta(x_1 - x_2), \quad (3)$$

where x_k is the position of the k -th atom. The trapping potential V is modeled by a piecewise harmonic triple well [5] with minima located at d_L , d_M , and d_R (see Fig. 1(a)). The last term describes the contact interaction (of strength g) between the atoms [26].

From here on, we refer to the ground state of two interacting bosons in each harmonic well as $|j\rangle$ ($j = L, M, R$), whose energy E_g is related to g by [26]

$$g = -\frac{2\sqrt{2}\Gamma(1 - E_g/2)}{\Gamma((1 - E_g)/2)}, \quad (4)$$

where $\Gamma(x)$ is the gamma function. Throughout the paper we will discuss the whole range of E_g : from the non-interacting case ($g = 0$, $E_g = 1$) to the Tonks-Girardeau (TG) limit ($g \rightarrow \infty$, $E_g = 2$). Our objective

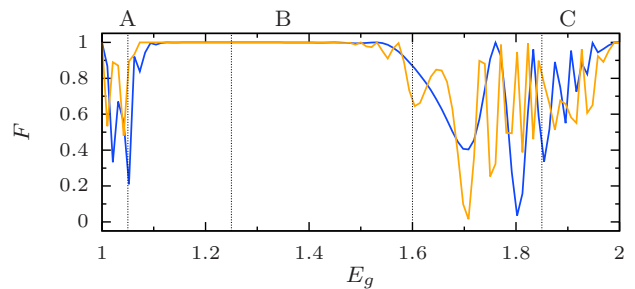


FIG. 2. (Color online) Final population in state $|R\rangle$ as a function of E_g after the two-particle SAP protocol is carried out over a total time $T = 4000$ (blue/dark gray) or $T = 12000$ (orange/light gray). Dotted vertical lines indicate energies for which the spectrum is shown in Figs. 3 and 4.

is to find an eigenstate of H , analogous to the single-particle dark state (tending to $|L\rangle$ and $|R\rangle$ at initial and final times) which allows for two-particle SAP transport between these states.

IV. SAP FOR INTERACTING PARTICLES

With the system initially in state $|L\rangle$, we numerically integrate the time-dependent Schrödinger equation with the Hamiltonian (3) while changing the positions of the traps as shown in Fig. 1(a). We then calculate the SAP fidelity F (population of $|R\rangle$ at final time $t = T$) for E_g between 1 and 2. The results for two different values of T are shown in Fig. 2, where one can identify several regions of interest.

The process succeeds for the non-interacting case ($E_g = 1$), where the particles are independent and each undergoes single-particle SAP. Full transfer also occurs in the TG limit ($E_g = 2$), which can be easily understood since the bosonic atoms can be treated as independent fermions occupying the two lowest single-particle energy levels, and each of them can then be treated with a Hamiltonian similar to Eq. (1) [9]. The fidelity drops sharply for energies near these extreme values, regions A and C in Fig. 2, where the population transfer is only partial and depends on T . However, from $E_g \simeq 1.12$ to $E_g \simeq 1.45$ (region B) a plateau appears where $F > 0.998$.

In the rest of this work, we will analyze these three regions in detail by diagonalizing the exact Hamiltonian of the system. We will also introduce two Hubbard Hamiltonians, for weak and strong interactions, whose formalism will allow us to study the structure of the eigenstates and give additional insight into the importance of co-tunneling processes.

V. WEAK INTERACTIONS

Restricting the analysis to two-particle states in the lowest Bloch band, the system can be modeled for weak interactions using a finite-size Bose–Hubbard Hamiltonian [27]

$$H_B = \sum_{j=L,M,R} \left[\frac{U}{2} n_j(n_j - 1) + \epsilon_0 n_j \right] \quad (5)$$

$$+ \Omega_{LM} (b_L^\dagger b_M + b_M^\dagger b_L) + \Omega_{MR} (b_M^\dagger b_R + b_R^\dagger b_M)$$

$$+ \Omega_{LM}^{(\text{co})} (b_L^{\dagger 2} b_M^2 + b_M^{\dagger 2} b_L^2) + \Omega_{MR}^{(\text{co})} (b_M^{\dagger 2} b_R^2 + b_R^{\dagger 2} b_M^2),$$

where b_j^\dagger and b_j are the creation and annihilation operators for a boson in the ground state of well j and $n_j = b_j^\dagger b_j$ is the number operator. The onsite interaction is described by U and the ground state energy is $\epsilon_0 = 1/2$. Single-particle tunneling rates ($\Omega_{jj'}$) and two-particle co-tunneling rates ($\Omega_{jj'}^{(\text{co})}$) between wells j and j' are numerically calculated via the Gram–Schmidt orthonormalization procedure [9] using the single-particle [5] and two-particle [26] wave functions, respectively.

When the two traps are close to each other, $\Omega_{jj'}$ and $\Omega_{jj'}^{(\text{co})}$ are of the same order of magnitude, but for weak interactions single-particle tunneling dominates due to its larger amplitude. For stronger interactions, however, single-particle tunneling becomes off-resonant, unlike co-tunneling which dominates because it remains resonant. While co-tunneling is not usually considered, it is crucial to understand the behavior observed in the previous section. A study of H_B (with real-time simulations, eigenvalues and eigenstates) with and without co-tunneling terms can be found in the appendix.

In order to understand regions A and B in Fig. 2 we diagonalize numerically both H and H_B at any point during the SAP evolution. The spectra of H for $E_g = 1.05$ and 1.25 are shown in Fig. 3(a,b), and consist of three distinct bands. The lowest band contains three states (where the two atoms sit in different wells), and for large trap separations (i.e., initial and final times) has energy 1. Not discussed here, this band contains an eigenstate which allows the adiabatic transfer of an atomic hole between the outermost wells for strong enough interactions [16]. The middle band (also with three states) is the one of interest to us because it only involves states with the two atoms in the same trap, $|j\rangle$, with energies around $1 + U = E_g$. The higher band, with energies around 2, consists of six states which correspond to states where the atoms sit in the ground state and first excited states of different traps. For the same parameters, the spectrum of H_B is shown in Fig. 3(c,d). These spectra show two bands, corresponding (with good agreement) to the two lower bands of the exact Hamiltonian we have just discussed. Higher bands do not appear because only the lowest Bloch band has been considered in H_B .

The band around E_g has a similar structure to the single-particle SAP spectrum (cf. Fig. 1(b)) and it

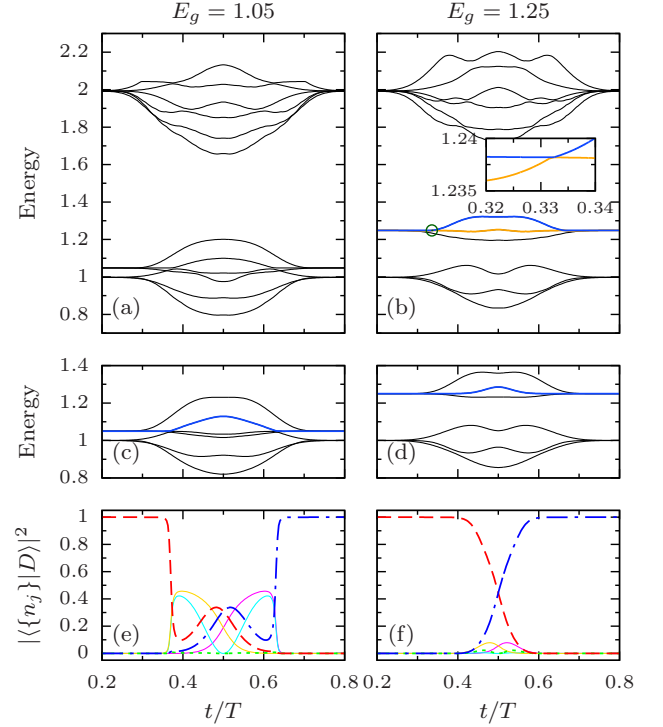


FIG. 3. (Color online) (a,b) Lowest 12 eigenvalues of H for the two-particle SAP scheme with the trap moving sequence of Fig. 1(a) for (a) $E_g = 1.05$ and (b) $E_g = 1.25$. In (b) the energy of the dark state (asymptotically $|L\rangle$ and $|R\rangle$) and the state with which it couples the most are marked in blue (dark gray) and orange (light gray), respectively. The inset shows a zoom-in of the marked crossing between these two states (marked with a circle) which is analyzed in Sec. VII. (c,d) Eigenvalues of H_B for the same parameters as (a,b), with the energy of the dark state drawn in blue (gray). (e,f) Coefficients in the Fock basis $|\{n_j\}\rangle$ of the dark states in (c,d) (dashed red corresponds to $|L\rangle$, dotted green to $|M\rangle$, dot-dashed blue to $|R\rangle$, and the solid lines to states where the two atoms are in different traps).

contains an eigenstate, drawn in blue (dark gray) in Fig. 3(c,d), which allows for SAP transport because of its dark-state-like structure, shown in Fig. 3(e,f). It is important to remark that this state is only present if co-tunneling is considered in H_B , see the appendix. The SAP transport fails for weak interactions, Fig. 3(a,c,e), because when tunneling becomes relevant the two bands overlap and dynamically following the dark state is hard due to the presence of level crossings. We can then see that the appearance of the plateau in Fig. 2 for stronger interactions, i.e., $U \gtrsim \sqrt{2}\Omega \sim 0.15$, is due to the two bands remaining separated during the whole process, see Fig. 3(b,d). This allows for the SAP process to be successful again because the band with the dark state resembles the single-particle SAP spectrum, cf. Fig. 1(b). The dark state has a similar shape to the single-particle one but for the states $|j\rangle$ coupled through co-tunneling (compare Figs. 3(f) and 1(c)).

VI. STRONG INTERACTIONS

One expects then that for stronger interactions the process will keep working, until E_g approaches the band with energies around 2, which will cause the fidelity to drop again in region C of Fig. 2. Because of the fermionic behavior of the TG gas, this regime is best modeled by restricting the system to two-particle Fock states with one atom in each of the two lowest Bloch bands and using a finite-size Fermi–Hubbard Hamiltonian [27]

$$\begin{aligned}
 H_F = & \sum_{j=L,M,R} \left[U n_{j0} n_{j1} + \sum_{i=0,1} \epsilon_i n_{ji} \right] \\
 & + \sum_{i=0,1} \left[\Omega_{LM}^{(i)} a_{L0}^\dagger a_{M1} + \Omega_{MR}^{(i)} a_{M0}^\dagger a_{R1} + \text{h.c.} \right] \\
 & + \Omega_{LM}^{(\text{co})} a_{L0}^\dagger a_{L1}^\dagger a_{M0} a_{M1} + \text{h.c.} \\
 & + \Omega_{MR}^{(\text{co})} a_{M0}^\dagger a_{M1}^\dagger a_{R0} a_{R1} + \text{h.c.}
 \end{aligned} \quad (6)$$

Here a_{ji}^\dagger and a_{ji} are the fermionic creation and annihilation operators for a particle at energy level i of well j , $\Omega_{jj'}^{(i)}$ are the tunneling frequencies at level i , $n_{ji} = a_{ji}^\dagger a_{ji}$, and $\epsilon_i = 1/2 + i$. The onsite interaction is given by U , which is now negative since two bosons interacting repulsively with finite strength have less energy than two non-interacting fermions. In other words, the ground state energy is now $\epsilon_0 + \epsilon_1 + U = 2 - |U| = E_g$.

We show in Fig. 4(a,b) the spectrum of H for $E_g = 1.6$ and 1.85, and one can see the same three-band structure as in Fig. 3. For the same values of E_g , the spectrum of H_F , Fig. 4(c,d), consists of two bands: around $2 - |U| = E_g$ and 2, in good agreement with the exact results. Once again, one state in the band around E_g (in blue/gray) has the form of a dark state, see Fig. 4(e,f). As E_g increases, the two bands start to overlap and crossings appear, leading to the dark state involving states of the upper band, see Fig. 4(b,d), which perturb the adiabatic transfer as seen in region C. It is worth noting that H_F contains a dark state even without the co-tunneling term.

VII. (A)DIABATIC REQUIREMENTS

Thus far we have seen that our system's Hamiltonian contains a band with energies around E_g which consists of a three-level system of states $|j\rangle$, coupled by repulsively-bound pair tunneling. Thanks to the atomic interaction, this band can be isolated from the rest of two-particle states, and allows the transport to succeed. From the size of the two bands of H_F , one would expect that process should not be affected by level crossings until around $E_g \sim 1.7$. However, the plateau in Fig. 2 only extends until $E_g \sim 1.5$. In order to understand this we will look back on the spectrum of the exact Hamiltonian spectra in Figs. 3(b) and 4(a). For both spectra we have highlighted

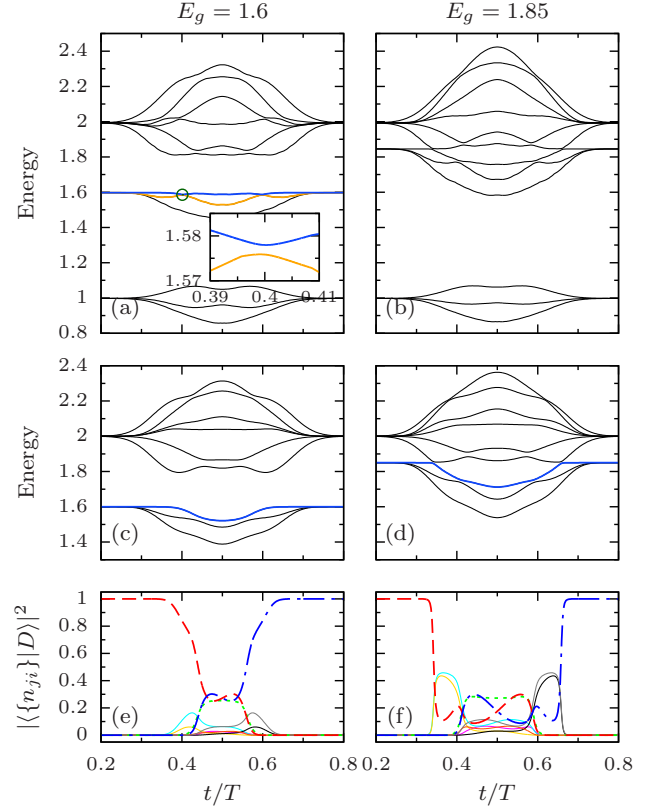


FIG. 4. (Color online) (a,b) Lowest 12 eigenvalues of H for the two-particle SAP scheme with the trap moving sequence of Fig. 1(a) for (a) $E_g = 1.6$ and (b) $E_g = 1.85$. In (a) the energy of the dark state (asymptotically $|L\rangle$ and $|R\rangle$) and the state with which it couples the most are marked in blue (dark gray) and orange (light gray), respectively. The inset shows a zoom-in of the marked crossing between two states (marked with a circle) which is analyzed in Sec. VII. (c,d) Eigenvalues of H_F for the same parameters as (a,b), with the energy of the dark state drawn in blue (gray). (e,f) Coefficients of the dark state in (c,d) the Fock basis $|\{n_{ji}\}\rangle$ (color coding is the same as in Figs. 3(e,f)).

in blue (dark gray) the energy of the dark state, i.e., the state which at initial and final times is $|L\rangle$ and $|R\rangle$, respectively, and therefore the state we are initially following. In contrast to the Hubbard Hamiltonians, this dark state crosses another eigenstate (shown in orange/light gray) twice, creating a finite probability for the system to leave the dark state. For $1.1 \lesssim E_g \lesssim 1.8$ these are the only relevant crossings affecting the dark state, and we examine them carefully in the following. However, as the crossings are actually avoided crossings, it is clear that the speed at which they are passed will determine the adiabaticity and the success of the transfer [28, 29].

The probability for a system following an eigenvector $|i(t)\rangle$ to be excited into another one $|j(t)\rangle$ between times

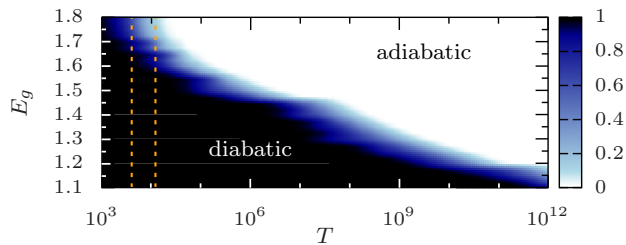


FIG. 5. (Color online) Probability of transition $p_{i \rightarrow j}$ at the crossing between the eigenstates shown in the insets of Figs. 3 and 4 for different total times T and energies E_g . Dashed vertical lines indicate the total times used in Fig. 2.

t_0 and t_f can be approximated by [30]

$$p_{i \rightarrow j} \simeq \frac{\left| \int_{t_0}^{t_f} \langle j(t) | \frac{d}{dt} | i(t) \rangle e^{i \int_{t_0}^t (E_j(\tau) - E_i(\tau)) d\tau} dt \right|^2}{\left| \int_{t_0}^{t_f} \langle j(t) | \frac{d}{dt} | i(t) \rangle dt \right|^2}, \quad (7)$$

where $E_k(t)$ is the energy of state $|k(t)\rangle$. The denominator was added from the original expression for normalization purposes and represents the probability for the state to be excited for an infinitely fast process. Full transfer through the SAP protocol can be achieved if both crossings are passed either adiabatically ($p_{i \rightarrow j} = 0$, following always the dark state) or completely diabatically ($p_{i \rightarrow j} = 1$, following the orange (light gray) state between the crossings). For intermediate values of $p_{i \rightarrow j}$, the system's actual state will be distributed between different eigenstates and the transfer will not be complete.

In Fig. 5 we show the calculated transition probabilities for the gap as a function of T and E_g . One can see that for the timescales of T used in Fig. 2, the transfer is completely diabatic for $E_g = 1.25$. For $E_g = 1.6$, however, $p_{i \rightarrow j}$ starts to fall to 0.99 (0.96) for $T = 4000$ (12000), and even lower for higher E_g . Therefore, the plateau ends because of the increased size of the gap in the avoided crossing, which no longer allows for diabatic passage. Moreover, it can be seen that the length and position of the plateau is T -dependent, since the transition from a diabatic to an adiabatic process happens at very different time scales, which depend on E_g . For longer time scales, e.g. of the order of 10^7 , two plateaus would appear in region B: one from $E_g \sim 1.1$ – 1.4 in which the transfer in this crossing would be completely diabatic, and one at $E_g \sim 1.5$ – 1.7 where the transfer would be adiabatic.

VIII. CONCLUSION

In this work we have studied the spatial adiabatic passage protocol for a system of interacting bosons over the entire range of repulsive interactions. We have found that, in addition to the trivial cases for non-interacting and infinitely strongly interacting particles, a large and

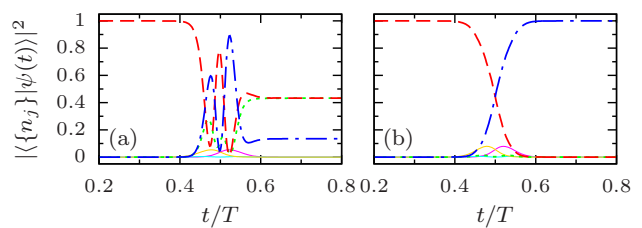


FIG. 6. (Color online) Populations of the eigenstates from integrating the Schrödinger equation with the Hamiltonian H_B for $E_g = 1.25$ (a) without and (b) with the co-tunneling terms. The initial state is $|\psi(t=0)\rangle = |L\rangle$ and the tunneling rates are calculated numerically with the time-dependent trap positions in Fig. 1(a). Color coding is the same as in Figs. 3(e,f).

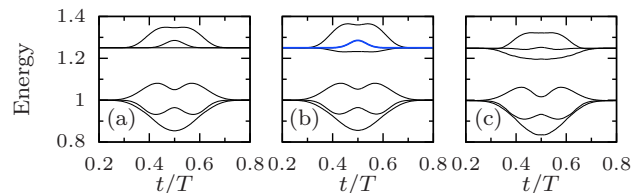


FIG. 7. (Color online) Spectra of (a) the exact Hamiltonian (lowest six eigenstates), and H_B without (b) and with (c) the co-tunneling terms for the SAP process as a function of time for $E_g = 1.25$ ($U = 0.25$). The energy of the dark state in (b) is shown in blue (gray).

continuous region for intermediate interactions exist over which high fidelities can be obtained. This is due to the fact that for intermediate values of E_g a decoupled energy band appears, which possess a dark state facilitated by two-particle co-tunneling. However, when this band overlaps with other energy bands, the appearance of level crossings prevents the robust use of the dark state. This behavior is generic to any multi-well setting and not specific to SAP. It is worth noting that the above effect is limited to systems where no phonon modes exist and therefore does, for example, not apply to SAP in quantum dot systems.

ACKNOWLEDGMENTS

This work was supported by the Okinawa Institute of Science and Technology Graduate University. We thank Irina Reshodko for helpful discussions.

APPENDIX: JUSTIFICATION OF THE CO-TUNNELING TERMS

In this appendix we will examine the validity of the Bose-Hubbard Hamiltonian in greater detail and confirm the importance of the co-tunneling terms. For this

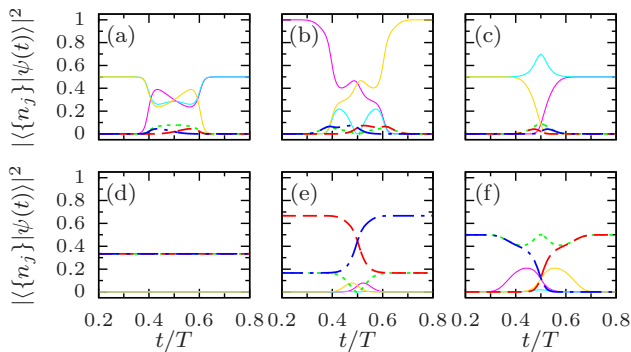


FIG. 8. (Color online) Populations of the eigenstates of the H_B without the co-tunneling terms in the Fock basis for the SAP process as a function of time. States are ordered with increasing energy as (a) to (f), and use the same color coding as Figs. 3(e,f).

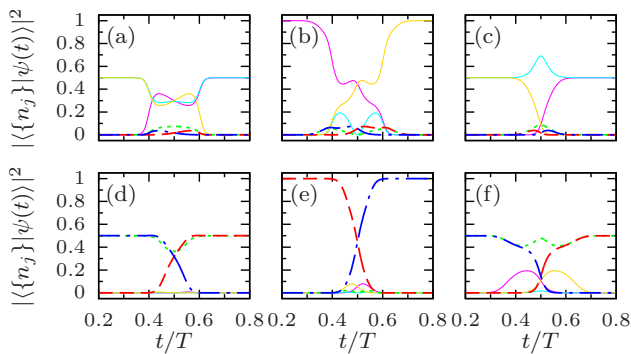


FIG. 9. (Color online) Same as Fig. 8 but including the co-tunneling terms in H_B .

we have performed numerical simulations of the time-

dependent Schrödinger equation using H_B for $E_g = 1.25$ ($U = 0.25$) and, because this falls inside region B of Fig. 2, the process is expected to work. The results, shown in Fig. 6, compare the cases where the co-tunneling terms in Eq. (5) are either neglected or considered and one can immediately notice that the simulation that does not consider the co-tunneling terms gives incomplete transfer to state $|R\rangle$. However, when one considers the co-tunneling terms, the transfer is complete, which establishes that these terms are crucial in order to explain the two-particle dynamics.

To shed more light on this we have also computed the spectrum of H_B , without and with co-tunneling, and that of the exact Hamiltonian during SAP. The results are shown in Fig. 7, and one can see that the inclusion of the co-tunneling terms leads to H_B approximating the exact spectrum more closely. Furthermore, we have computed the populations of the eigenstates in the Fock basis without (Fig. 8) and with (Fig. 9) co-tunneling terms. States in the lower band, depicted in (a-c), are mostly composed by states where the atoms are in separate traps. Because these states do not couple through co-tunneling, both their structure and energies coincide in Figs. 8 and 9. It is noteworthy that the state in (b) corresponds to another kind of dark state that transfers an atomic hole from the right well to the left well [15]. The states in the higher band, shown in (d-f), clearly differ for the two Hamiltonians. When the co-tunneling terms are absent, no dark state that allows transitions from $|L\rangle$ to $|R\rangle$ exists in H_B , see Fig. 8. However, it is clearly present when taking into account co-tunneling, see Fig. 9(e) (the energy of the dark state is shown in blue (gray) in Fig. 7(b)).

Therefore we have clearly established that a dark state that allows transfer between $|L\rangle$ and $|R\rangle$ is only present in H_B if the co-tunneling terms are considered.

-
- [1] D. Jaksch, H.-J. Briegel, J. I. Cirac, C. W. Gardiner, and P. Zoller, *Entanglement of atoms via cold controlled collisions*, Phys. Rev. Lett. **82**, 1975 (1999).
 - [2] A. Sørensen, L.-M. Duan, J. I. Cirac, and P. Zoller, *Many-particle entanglement with Bose-Einstein condensates*, Nature **409**, 63 (2001).
 - [3] S. Murmann, A. Bergschneider, V. M. Klinkhamer, G. Zürn, T. Lompe, and S. Jochim, *Two fermions in a double well: Exploring a fundamental building block of the Hubbard model*, Phys. Rev. Lett. **114**, 080402 (2015).
 - [4] L. Cao and I. Brouzos and S. Zöllner, and P. Schmelcher, *Interaction-driven interband tunneling of bosons in the triple well*, New J. Phys. **13**, 033032 (2011).
 - [5] K. Eckert, M. Lewenstein, R. Corbalán, G. Birkel, W. Ertmer, and J. Mompert, *Three-level atom optics via the tunneling interaction*, Phys. Rev. A **70**, 023606 (2004).
 - [6] A. D. Greentree, J. H. Cole, A. R. Hamilton, and L. C. L. Hollenberg, *Coherent electronic transfer in quantum dot systems using adiabatic passage*, Phys. Rev. B **70**, 235317 (2004).
 - [7] S. Longhi, *Adiabatic passage of light in coupled optical waveguides*, Phys. Rev. E **73**, 026607 (2006).
 - [8] R. Menchon-Enrich, J. Mompert, and V. Ahufinger, *Spatial adiabatic passage processes in sonic crystals with linear defects*, Phys. Rev. B **89**, 094304 (2014).
 - [9] Y. Loiko, V. Ahufinger, R. Corbalán, G. Birkel, and J. Mompert, *Filtering of matter-wave vibrational states via spatial adiabatic passage*, Phys. Rev. A **83**, 033629 (2011).
 - [10] T. Morgan, L. J. O’Riordan, N. Crowley, B. O’Sullivan, and Th. Busch, *Coherent transport by adiabatic passage on atom chips*, Phys. Rev. A **88**, 053618 (2013).
 - [11] R. Menchon-Enrich, S. McEndoo, J. Mompert, V. Ahufinger and Th. Busch, *Tunneling-induced angular momentum for single cold atoms*, Phys. Rev. A **89**, 013626 (2014).
 - [12] E. M. Graefe, H. J. Korsch, and D. Witthaut, *Mean-field dynamics of a Bose-Einstein condensate in a time-dependent triple-well trap: Nonlinear eigenstates, Landau-Zener models, and stimulated Raman adiabatic*

- passage, Phys. Rev. A **73**, 013617 (2006).
- [13] M. Rab, J. H. Cole, N. G. Parker, A. D. Greentree, L. C. L. Hollenberg, and A. M. Martin, *Spatial coherent transport of interacting dilute Bose gases*, Phys. Rev. A **77**, 061602(R) (2008).
 - [14] C. J. Bradley, M. Rab, A. D. Greentree, and A. M. Martin, *Coherent tunneling via adiabatic passage in a three-well Bose-Hubbard system*, Phys. Rev. A **85**, 053609 (2012).
 - [15] A. Benseny, J. Bagudà, X. Oriols, and J. Mompart, *Need for relativistic corrections in the analysis of spatial adiabatic passage of matter waves*, Phys. Rev. A **85**, 053619 (2012).
 - [16] A. Benseny, S. Fernández-Vidal, J. Bagudà, R. Corbalán, A. Picón, L. Roso, G. Birkel, and J. Mompart, *Atomtronics with holes: Coherent transport of an empty site in a triple-well potential*, Phys. Rev. A **82**, 013604 (2010).
 - [17] K. Winkler, G. Thalhammer, F. Lang, R. Grimm, J. Hecker-Denschlag, A. J. Daley, A. Kantian, H. P. Büchler, and P. Zoller, *Repulsively bound atom pairs in an optical lattice*, Nature **441**, 853 (2006).
 - [18] S. Zöllner, H.-D. Meyer, and P. Schmelcher, *Tunneling dynamics of a few bosons in a double well*, Phys. Rev. A **78**, 013621 (2008).
 - [19] J. C. Amadon and J. E. Hirsch, *Metallic ferromagnetism in a single-band model: Effect of band filling and Coulomb interactions*, Phys. Rev. B **54**, 6364 (1996).
 - [20] G. Mazzaella, S. M. Giampaolo, and F. Illuminati, *Extended Bose-Hubbard model of interacting bosonic atoms in optical lattices: From superfluidity to density waves*, Phys. Rev. A **73**, 013625 (2006).
 - [21] U. Bissbort, F. Deuretzbacher, and W. Hofstetter, *Effective multibody-induced tunneling and interactions in the Bose-Hubbard model of the lowest dressed band of an optical lattice*, Phys. Rev. A **86**, 023617 (2012).
 - [22] D.-S. Lühmann, O. Jürgensen, and K. Sengstock, *Multi-orbital and density-induced tunneling of bosons in optical lattices*, New J. Phys. **14**, 033021 (2012).
 - [23] M. Maik, P. Hauke, O. Dutta, M. Lewenstein, and J. Zakrzewski, *Density-dependent tunneling in the extended Bose-Hubbard model*, New J. Phys. **15**, 113041 (2013).
 - [24] W. Ganczarek, M. Modugno, G. Pettini, and J. Zakrzewski, *Wannier functions for one-dimensional s-p optical superlattices*, Phys. Rev. A **90**, 033621 (2014).
 - [25] K. Bergmann and H. Theuer, and B. W. Shore, *Coherent population transfer among quantum states of atoms and molecules*, Rev. Mod. Phys. **70**, 1003 (1998).
 - [26] Th. Busch, B.-G. Englert, K. Rzażewski, and M. Wilkens, *Two cold atoms in a harmonic trap*, Found. Phys. **28**, 549 (1998).
 - [27] D. Jaksch and P. Zoller, *The cold atom Hubbard toolbox*, Ann. Phys. **315**, 52 (2005).
 - [28] L. D. Landau and L. M. Lifshitz, *Quantum mechanics (non-relativistic theory), volume 3 (third edition)*, Butterworth-Heinemann (1981).
 - [29] K. Härkönen, O. Kärki, and K.-A. Suominen, *Tailoring of motional states in double-well potentials by time-dependent processes*, Phys. Rev. A **74**, 043404 (2006).
 - [30] A. Messiah, *Quantum mechanics, volume II*, Elsevier Science B. V. (1961).